

Optical properties of Cu nanoclusters supported on MgO(100)

Annalisa Del Vitto

Dipartimento di Scienza dei Materiali, Università di Milano-Bicocca, via R. Cozzi 53, I-20125 Milano, Italy

Carmen Sousa and Francesc Illas

Departament de Química Física i Centre de Recerca en Química Teòrica, Universitat de Barcelona i Parc Científic de Barcelona, C/Martí i Franquès 1, E-08028 Barcelona, Spain

Gianfranco Pacchioni^{a)}

Dipartimento di Scienza dei Materiali, Università di Milano-Bicocca, via R. Cozzi 53, I-20125 Milano, Italy

(Received 27 May 2004; accepted 30 July 2004)

The vertical transitions of Cu atoms, dimers, and tetramers deposited on the MgO surface have been investigated by means of *ab initio* calculations based either on complete active space second-order perturbation theory or on time-dependent density functional theory. Three adsorption sites have been considered as representative of the complexity of the MgO surface: regular sites at flat (100) terraces, extended defects such as monoatomic steps, and point defects such as neutral oxygen vacancies (F or color centers). The optical properties of the supported Cu clusters have been compared with those of the corresponding gas-phase units. Upon deposition a substantial modification of the energy levels of the supported cluster is induced by the Pauli repulsion with the substrate. This causes shifts in the optical transitions going from free to supported clusters. The changes in cluster geometry induced by the substrate have a much smaller effect on the optical absorption bands. On F centers the presence of filled impurity levels in the band gap of MgO results in a strong mixing with the empty levels of the Cu atoms and clusters with consequent deep changes in the optical properties of the color centers. The results allow to interpret electron energy loss spectra of Cu atoms deposited on MgO thin films. © 2004 American Institute of Physics.
[DOI: 10.1063/1.1796311]

I. INTRODUCTION

Metal nanoclusters on oxides are attracting an increasing interest for their potential impact in high-technological areas like magnetic recording, optical properties, chemical reactivity on monodispersed catalysts, etc.¹ The chemical properties of supported nanoclusters deposited on oxide surfaces and thin films and their potential use as model catalysts have been studied in detail, while the number of studies dealing with magnetic and optical properties of deposited nanoparticles is scarce. Metal clusters on oxides are generally produced by self-assembling of deposited atoms from a metal vapor.¹ It is now quite well accepted that the nucleation and growth of the metal aggregates occurs on point defects where the diffusion of the atoms is inhibited by the strong interaction with the substrate. On these sites the formation of dimers and clusters has a much higher probability to occur than on regular sites. Also when clusters are produced in a molecular beam, mass selected, and deposited by soft-landing techniques on oxide substrates, the clusters diffuse on the surface until they become anchored to a point or an extended defect.^{2,3} Atoms and clusters diffusion is inhibited only at very low temperatures. The interaction with the defect can modify significantly the properties of the deposited cluster. For instance, it has been shown that a charge transfer occurs from oxygen vacancies on ionic surfaces, such as

MgO, to a supported metal cluster and that this charge transfer can turn an inactive species into an active catalyst.⁴ Thus, going from a gas-phase cluster to a deposited one it is possible to induce major modifications of its electronic and geometrical properties, in particular when the interaction with the substrate involves a point defect. The interaction with point defects is completely screened for large metal particles of a few nanometer size, containing hundreds of atoms, while is important for truly nanoclusters containing up to about ten atoms.⁵

Small metal particles absorb light giving rise to collective excitations of electrons (plasmon excitation) described by Mie theory.⁶ For a spherical gas-phase particle a single Mie resonance is expected, but when the particle is deposited on a substrate its shape changes from spherical to an ellipsoid and two different resonances are expected, with excitation dipole normal and parallel to the surface, respectively. This has been observed recently for Ag particles of 2–3 nm size deposited on mica, showing the effect of the substrate interaction on the plasmon excitation of a cluster.⁷ However, when the particle size decreases and becomes <1 nm electrons do not behave any more according to the classical Mie theory and their transitions must be described with the laws of quantum mechanics, thus taking explicitly into account the quantized nature of the energy levels. This opens in principle the possibility to manipulate the optical properties as a function of the cluster size, of the constituting elements, of the substrate where it is deposited, of the point defect where it is stabilized, etc. The detailed knowledge of the factors

^{a)} Author to whom correspondence should be addressed. Electronic mail: Gianfranco.pacchioni@unimib.it

which affect the optical transitions of a nanocluster is thus essential to design materials with desired optical response.⁸ Very few studies have been reported so far on the optical properties of supported nanoclusters. Two of these studies have been dealing with Cu and Ag atoms and clusters on MgO thin films,^{9,10} thus motivating a theoretical study on this topic.

In this paper we report results of state-of-the-art electronic structure calculations on the optical properties of Cu atoms, dimers, and tetramers deposited on various sites of the MgO surface. The determination of the ground-state geometry of the clusters adsorbed on regular sites, extended defects (steps), and on point defects like a neutral oxygen vacancy (F centers) has been done by means of gradient corrected density functional theory (DFT) calculations. The determination of the transition energies and intensities has been done at the time-dependent DFT (TD-DFT) level, and the results have been checked for small systems using a wave function based multireference second-order perturbation theory method. The results show that the changes in optical transitions of Cu dimers or tetramers supported on MgO are not due to the modest changes in the cluster geometry but to the interaction with the substrate. This is particularly important for F centers which deeply modify the ordering and the nature of the levels involved in the cluster optical transitions.

II. COMPUTATIONAL DETAILS

The vertical transitions of Cu_n clusters ($n = 1, 2, 4$) in gas phase and supported on the MgO(100) surface have been determined at the TD-DFT level.¹¹ To confirm the validity of the TD-DFT results, some of the transitions have been studied also using the complete active space second-order perturbation theory^{12,13} (CASPT2) method. This approach has been restricted to free and supported Cu monomers and dimers. The calculation of the ground-state properties and optimal geometry has been done using a DFT approach based on the hybrid B3LYP functional,¹⁴ where the Hartree Fock (HF) exchange is mixed in with the DFT exchange using the Becke three-parameter approach combined with the nonlocal expression of the correlation functional proposed by Lee, Yang, and Parr.¹⁵ This is also the functional adopted for the TD-DFT calculations.

TD-DFT is based on the Kohn-Sham formulation of DFT and uses the eigenvalues and eigenvectors of the Kohn-Sham equation. The excitation energies are calculated from the poles of the frequency-dependent polarizability and the oscillator strengths from the residues. Recent studies have shown that TD-DFT can be more accurate than the configuration interaction single method,¹⁶ and that it can provide transition energies with accuracy similar to that of multireference configuration interaction (MRCI) or coupled-cluster methods.¹⁷ The TD-DFT approach starts to provide inaccurate results for transitions to states close to or in the conduction band of a solid material.¹⁷ For this reason, our investigation is restricted to the lowest two excitations allowed by spin selection rules.

CASPT2 is a generalization to complete active space self-consistent field (CASSCF) wave functions of the well-known second-order Møller-Plesset perturbation scheme

(MP2) based on closed-shell HF reference wave functions, and reduces rigorously to MP2 for CAS containing a single closed-shell Slater determinant. An important part of the nondynamical electron correlation effects is treated variationally in the CASSCF step, and the remainder, mainly dynamical electron correlation, is estimated by second-order perturbation theory with the CASSCF as zeroth-order wave function. This strategy combines the accuracy of a multireference configuration interaction treatment and the low computational cost of a perturbational approach. The method has been successfully applied to study excited states in solid state compounds.^{18–21} For Cu monomers the active space used includes 11 electrons in 12 orbitals, the $3d$, $4s$, and one of the $4p$ orbitals plus an extra set of virtual orbitals mainly of d character. It has been shown that for cases where the d shell is more than half occupied the inclusion of this extra set of virtual orbitals in the active space is necessary to properly account for nondynamical correlation effects of the d electrons.¹⁸ Moreover, for Cu interacting with a F center, two additional electrons and two additional orbitals (the s -like and p -like orbitals of the oxygen vacancy) were also included in the active space. For the dimers the active space contains ten electrons in ten orbitals which are the σ components of the $3d$ orbitals, their virtual counterparts and the bonding and antibonding orbitals resulting from the combination of the Cu($4s$) orbitals. The CASSCF/CASPT2 calculations have been performed using the MOLCAS 5 package.²²

The MgO surface has been represented using an embedded cluster model approach.²³ A large matrix of point charges (± 2) placed at the lattice positions around the cluster reproduces with sufficient accuracy the long-range Madelung field.²⁴ The positive charges at the cluster borders have been replaced by effective core potentials (ECP) to take into account the finite size of the Mg^{2+} core and prevent an artificial polarization of oxide anions.²⁵ Since the Cu-MgO interaction takes place essentially above oxygen anions,^{26–30} the adsorption sites have been represented by the cluster models centered on oxygen. These are $\text{O}_9\text{Mg}_9\text{ECP}_{16}$ for Cu and Cu_2 and $\text{O}_{13}\text{Mg}_{13}\text{ECP}_{16}$ for Cu_4 adsorbed on a MgO terrace (O_{5c}); $\text{O}_{10}\text{Mg}_{10}\text{ECP}_{13}$ for Cu and Cu_2 and $\text{O}_{15}\text{Mg}_{15}\text{ECP}_{20}$ for Cu_4 adsorbed on a MgO step site ($\text{O}_{4c}\text{-O}_{5c}$); $\text{O}_8\text{Mg}_9\text{ECP}_{16}$ for Cu and Cu_2 and $\text{O}_{12}\text{Mg}_{13}\text{ECP}_{16}$ for Cu_4 adsorbed on an oxygen vacancy located at the MgO terrace (F_{5c} center). In each case we have performed a geometry optimization by placing the Cu atom, dimer, or tetramer near an oxide anion or, for F centers, near the center of the vacancy, and by starting the optimization from various initial structures. For the small cluster models the substrate geometry was kept fixed to the truncated bulk for terrace and step sites, and to previously optimized structures for F centers. For the larger clusters all the atoms in the first layer which are not in direct contact with the embedding charges have been relaxed during the geometry optimization. However, details of the surface relaxation are not discussed since this is small and does not affect significantly the transition energies.

The Kohn-Sham orbitals have been expanded on a Gaussian-type atomic orbitals basis set. The Cu atoms were treated by a small core ECP which includes explicitly in the valence the $3s^2 3p^6 3d^{10} 4s^1$ electrons; the basis set is of

TABLE I. Adsorption energy (E_{ads}), shortest Cu-O distance, $r(\text{Cu-O}_{nc})$, vertical transition energies (T_e), and oscillator strengths (f) for free and MgO supported Cu atoms.

| | Cu ₁ Free | Cu ₁ /MgO(O _{5c}) Terrace | Cu ₁ /MgO(O _{4c}) Step | Cu ₁ /MgO(F _{5c}) Oxygen vacancy |
|---------------------------|--|--|--|--|
| E_{ads} (eV) | ... | 1.06 | 1.56 | 1.89 |
| $r(\text{Cu-O}_{nc})$ (Å) | ... | 2.229 | 1.928 | 3.442 ^a |
| 1st T_e (eV) | 1.38, 1.38, 1.38, 1.38, 1.38 [1.43] ^b | 2.29, 2.37, 2.37, 2.56, 2.57 [2.34,2.42,2.42, 2.67,2.69] ^b | 1.91 | 0.53, 0.69, 0.69 |
| f | 0.000 | 0.000 | 0.083 | 0.000 |
| Character | $3d^{10}4s^1 \rightarrow 3d^9 4s^2$ | $3d^{10}4s^1 \rightarrow 3d^9 4s^2$ | $4s \rightarrow 4p$ | $s(\text{F}_{5c}) \rightarrow p(\text{F}_{5c})$ |
| 2nd T_e (eV) | 3.89, 3.89, 3.89 [4.03] ^b | 2.63 | 2.53 | 1.94 |
| f | 0.270 | 0.115 | 0.105 | 0.134 |
| Character | $4s \rightarrow 4p$ | $4s \rightarrow 4p$ | $4s \rightarrow 4p$ | $s(\text{F}_{5c}) \rightarrow 4sp(\text{Cu}) + p(\text{F}_{5c})$ |

^aThis corresponds to a vertical distance of the Cu atom from the surface plane of 1.730 Å.

^bCASPT2 result.

double-zeta plus polarization type.³¹ The basis set employed for Mg and O atoms is 6-31G.³² The use of a larger 6-31+G* basis set on all the atoms of the O₉Mg₉ECP₁₆ cluster has been tested for the case of a single Cu atom. We found that the first five transition energies are shifted to higher values by 0.05–0.07 eV, with a change of 2% with respect to the smaller basis. When one oxygen atom is removed by the surface to form an F center one has to adopt a sufficiently flexible basis set to describe the electron localization in the vacancy: the solution adopted here is to use the diffuse 6-31+G basis set on the Mg ions surrounding the vacancy.³³ The binding energies E_{ads} of Cu clusters to MgO have not been corrected for the basis set superposition error (BSSE)³⁴ since this is not the main purpose of this paper. Furthermore, the definition of the BSSE reference energies

for adsorbed metal clusters that change their structure upon adsorption is not trivial.³⁵ A test calculation for the case of Cu atom adsorbed on a MgO terrace shows that the BSSE is 0.38 eV. Thus, one should keep in mind that all the adsorption energies reported in Tables I–III are overestimated. The calculations have been performed with the GAUSSIAN98 package for *ab initio* calculations.³⁶ For the CASSCF/CASPT2 calculations larger basis sets are generally required. Thus, for Cu and for the O atom directly interacting with Cu, the all electron Atomic Natural Orbital (ANO) ($21s\ 15p\ 10d\ 6f/7s\ 6p\ 5d\ 3f$) and ($14s\ 9p\ 4d/4s\ 3p\ 1d$) basis set have been employed, respectively, whereas for the rest of Mg and O atoms the ANO ($13s\ 8p/4s\ 3p$) and ($14s\ 9p/3s\ 2p$) sets have been used. For the F center an uncontracted ($3s, 2p, 1d$) has been placed at the center of the vacancy.³⁷

TABLE II. Adsorption energy (E_{ads}), dimer binding energy (E_b), Cu-Cu distance, $r(\text{Cu-Cu})$, binding energy per atom (D_e/at), vertical transition energies (T_e), and oscillator strengths (f) for free and MgO supported Cu dimers.

| | Cu ₂ Free | Cu ₂ /MgO(O _{5c}) Terrace | Cu ₂ /MgO(O _{4c}) Step | Cu ₂ /MgO(F _{5c}) Oxygen vacancy |
|-----------------------|--|--|--|--|
| E_{ads} (eV) | ... | 1.44 | 1.87 | 2.29 |
| E_b (eV) | ... | 1.33 | 1.17 | 1.35 |
| $r(\text{Cu-Cu})$ (Å) | 2.259 | 2.291 | 2.301 | 2.390 |
| D_e/at (eV) | 1.01 | 1.73 | 1.94 | 2.15 |
| 1st T_e (eV) | 2.53, 2.58, 2.58, 2.78, 2.78 [2.83] ^a | 2.95 | 2.83 | 2.00, 2.19, 2.19 |
| f | 0.000 | 0.126 | 0.141 | 0.000 |
| Character | $3d^{10}\sigma_g^2\sigma_u^{*0} \rightarrow 3d^9\sigma_g^2\sigma_u^{*1}$ | $\sigma_g \rightarrow \sigma_u^*$ | $\sigma_g \rightarrow \sigma_u^*$ | $s(\text{F}_{5c}) + \sigma_u^* \rightarrow p_z(\text{F}_{5c}), p_{x,y}(\text{F}_{5c})$ |
| 2nd T_e (eV) | 2.89 [2.49] ^a | 3.16, 3.16, 3.16, 3.17, 3.17 | 3.55 | 2.85 |
| f | 0.177 | 0.000 | 0.102 | 0.395 |
| Character | $\sigma_g \rightarrow \sigma_u^*$ | $3d^{10}\sigma_g^2\sigma_u^{*0} \rightarrow 3d^9\sigma_g^2\sigma_u^{*1}$ | $\sigma_g \rightarrow 4sp(\text{diffuse})$ | $s(\text{F}_{5c}) + \sigma_u^* \rightarrow p(\text{F}_{5c}) + 4sp(\text{diffuse})$ |

^aCASPT2 result.

TABLE III. Adsorption energy (E_{ads}), binding energy per atom (D_e/at), vertical transition energies (T_e), and oscillator strengths (f) for free and MgO supported Cu tetramers.

| | Cu ₄ Free | Cu ₄ /MgO(O _{5c}) Terrace | Cu ₄ /MgO(O _{4c}) Step | Cu ₄ /MgO(F _{5c}) Oxygen vacancy |
|----------------|---------------------------------------|---|--|--|
| E_{ads} (eV) | ... | 2.28 | 2.32 | 3.45 |
| D_e/at (eV) | 1.31 | 1.88 | 1.89 | 2.17 |
| 1st T_e (eV) | 1.19 | 1.76 | 1.42 | 1.92 |
| f | 0.000 | 0.006 | 0.000 | 0.000 |
| Character | $b_{3u}(4sp) \rightarrow b_{2u}(4sp)$ | $b_{3u}(4sp) \rightarrow b_{2u}(4sp)$ | $b_{3u}(4sp) \rightarrow$ $b_{2u}(4sp) + 3s(\text{Mg})$ | $s(\text{F}_{5c}) + b_{2u}(4sp) \rightarrow$ $s(\text{F}_{5c}) - b_{2u}(4sp)$ |
| 2nd T_e (eV) | 2.78, 2.79, 2.79, 2.80, 2.86 | 2.61 | 2.58 | 2.51 |
| f | 0.102 | 0.448 | 0.359 | 0.131 |
| Character | $3d \rightarrow b_{2u}(4sp)$ | $b_{3u}(4sp) \rightarrow b_{2u}(4sp)$ | $b_{3u}(4sp) \rightarrow$ $b_{2u}(4sp) + 3s(\text{Mg})$ | $s(\text{F}_{5c}) + b_{2u}(4sp) \rightarrow$ $s(\text{F}_{5c}) - b_{2u}(4sp)$ |

III. RESULTS AND DISCUSSION

A. Cu monomer

First, we consider the electronic transitions of a free Cu atom, Table I. Cu has a $[\text{Ar}]3d^{10}4s^1$ electronic configuration. The lowest excitation is of $^2S(3d^{10}4s^1) \rightarrow ^2D(3d^94s^2)$ type. CASPT2 predicts this transition to occur at 1.43 eV. In TD-DFT we find five degenerate states at 1.38 eV above the ground state characterized by the transition of one $3d$ electron to the partially filled $4s$ orbital. These transitions have zero oscillator strength as they are forbidden by selection rules. Nevertheless, it is known from atomic spectra that this transition occurs at 1.49 eV which corresponds to the weighted average of the spin-orbit levels.^{38,39} Within TD-DFT the space and spin symmetry is not defined and hence excitations are defined by the configuration change only. We find three allowed $4s^14p^0 \rightarrow 4s^04p^1$ excitations at 3.89 eV (TD-DFT) with $f=0.270$. These values are very close to the experimental value of 3.81 eV found for gas-phase Cu atoms, and assigned to the $4s^14p^0 \rightarrow 4s^04p^1$ excitation.^{38,39} The corresponding CASPT2 value is 4.03 eV.

When atomic copper is supported on MgO it binds preferentially to the oxygen anions of the surface or, if present, to oxygen vacancies.^{27,29} The results show that the Cu adsorption energy increases in the order $\text{O}_{5c} < \text{O}_{4c} < \text{F}_{5c}$, Table I. On the regular terrace Cu binds with an energy of 1.06 eV and a Cu-O distance of 2.23 Å, in agreement with previous results²⁶⁻³⁰ (notice that our adsorption energy is higher than previous estimates since no BSSE correction has been applied). The interaction with the surface perturbs the Cu electronic states, and shifts to higher energies the $4s$ level so that the $3d^{10}4s^1 \rightarrow 3d^94s^2$ excitation occurs now at 2.29 eV according to TD-DFT results (at this level, the same transition occurs at 1.38 eV in gas-phase, Table I). The result for the $3d^{10}4s^1 \rightarrow 3d^94s^2$ excitation in the supported Cu atom is confirmed by CASPT2 which gives a $T_e=2.34$ eV, very close to the TD-DFT value, Table I. This validates the use of TD-DFT for supported atoms and clusters. This transition however has no intensity and cannot be observed in optical absorption measurements. The destabilization of the Cu $4s$ level is a consequence of the Pauli repulsion with the sur-

face, and is also the reason for the relatively weak interaction with MgO. For the same reason, the gap between the $4s$ and the $4p$ related states is reduced for adsorbed Cu and the $4s^14p^0 \rightarrow 4s^04p^1$ excitation has a T_e of 2.63 eV, Table I, i.e., about 1.3 eV lower than in gas phase. Experimentally, the electron energy loss spectra (EELS) of thermally evaporated Cu atoms on MgO thin films at very low temperature (30 K) show an intense absorption at 2.7 eV followed by other absorptions at 3.9 and 5.1 eV.⁹ These transitions are clearly due to the deposited Cu atoms as no feature in this energy window is found for the clean MgO films. By comparison with transitions of Cu atoms and Cu^+ ions, the band at 2.7 eV has been assigned to a $3d^{10} \rightarrow 3d^94s^1$ excitation of Cu^+ and the band at 3.9 eV to the $4s \rightarrow 4p$ transition of neutral Cu atoms.^{9,10} Our results, on the contrary, provide strong support to the hypothesis that the transition at 2.7 eV observed experimentally is due to neutral Cu atoms and has $4s \rightarrow 4p$ character. It should be noticed, in addition, that the mechanism to create Cu^+ ions on the surface of a nonreducible oxide as MgO is unclear, unless major damage to the surface is produced in the phase of Cu atoms deposition. The $3d^{10} \rightarrow 3d^94s^1$ excitation of Cu^+ gives rise to two different transitions at 2.81 eV ($^1S \rightarrow ^3D$) and 3.26 eV ($^1S \rightarrow ^1D$);^{38,39} both are forbidden either because of spin or because of symmetry selection rules so that it is difficult to assign any of them to the very intense peak at 2.7 eV.

On a monoatomic step of MgO the Cu atom interacts with the O_{4c} site, $d(\text{O}_{4c}\text{-Cu})=1.93$ Å and $d(\text{O}_{5c}\text{-Cu})=3.58$ Å. The distance to the step atom is shorter, and the interaction is stronger, Table I, than on a terrace site. This causes a significant change in the position of the $4s$ and $4p$ levels of Cu, which are considerably mixed. The lowest excitation involves the $4s$ and $4p$ states and not the $3d$ ones. This means that the $3d^{10}4s^1 \rightarrow 3d^94s^2$ transition occurs at energies higher than 2.5 eV and is not included in our calculations. The first excitation is found at 1.91 eV and has $4s^14p^0 \rightarrow 4s^04p^1$ character, although the orbitals are strongly hybridized resulting in states exhibiting a mixed nature. The second excited state has similar character and appears at 2.53 eV, Table I. Both transitions at 1.91 and 2.53 eV have finite transition probabilities, Table I. The correspond-

ing excitation occurs at 3.89 eV in gas phase and at 2.63 eV on a MgO terrace. This means that the $4s$ states are progressively destabilized compared to the $4p$ one going from free Cu, to Cu on a terrace and on a step, reducing the $4s^1 4p^0 \rightarrow 4s^0 4p^1$ transition and increasing the $3d^{10} 4s^1 \rightarrow 3d^9 4s^2$ one. Thus, two allowed transitions at 1.9 and 2.5 eV are found for Cu atoms bound at steps. In the original spectrum of Schaffner *et al.*,^{9,10} for very low coverages of Cu, 0.06 ML, a relatively broad feature just above 2 eV is seen with more pronounced peaks at 2.4 and 2.7 eV. We suggest that the relatively broad feature in the EELS spectrum in the region 2.4–2.7 eV is due to Cu atoms adsorbed on both terrace and step sites. Notice that the low deposition temperature, 30 K, is such to prevent diffusion of the Cu atoms on the surface. Under these conditions, it is likely that the atoms remain close to the surface site where they have been deposited, thus being stabilized at flat terraces or eventually steps. By raising the temperature, it is known that metal atoms diffuse on the surface until they become trapped at point defects where the interaction with the substrate is much stronger.¹

F centers have specific optical properties connected to the presence of two electrons trapped in the cavity formed by removing the oxygen atom.⁴⁰ The two electrons occupy an s -like state of a_1 symmetry in the gap of MgO. We denote this state as $s(F_{5c})$. The lowest excitations on surface F centers occur around 3–3.5 eV according to *ab initio* calculations⁴¹ and EELS measurements on oxygen deficient MgO thin films.⁴² This transition involves states with $s(F_{5c})$ and $p(F_{5c})$ character, respectively.⁴¹ Therefore, F centers possess typical optical properties and excitations in an energy window which is not too far from that of the transitions of Cu atoms. The interaction of a Cu atom with an F center results in a vertical distance of Cu from the surface plane, $z_{\text{Cu}} = 1.73 \text{ \AA}$, shorter than in previous cases as the atom partially penetrates into the vacancy. The Cu $4s$ orbital strongly interacts with the $s(F_{5c})$ state of the F center forming a bonding and an antibonding combination where three electrons are accommodated, one from Cu and two from the F center. Since the $4s$ level is lower in energy, a charge transfer of one electron occurs from the F center to Cu, leaving a single electron into the $s(F_{5c})$ state. Above this level there are the p -type states of the vacancy of e and a_1 symmetry. The lowest excitations are thus from the singly occupied $s(F_{5c})$ level to the empty $p_{x,y}(F_{5c})$ and $p_z(F_{5c})$ states of the vacancy. They have no intensity and are rather low in energy, $T_e = 0.53\text{--}0.69 \text{ eV}$. However, these low energy excitations do not show up in CASPT2 calculations for Cu on F_{5c} . Considering that the nature of these transitions is not completely clarified and that they have no intensity, no particular meaning should be attributed to these excited states in the following discussion.

The first allowed transition, $f = 0.134$, occurs at 1.94 eV and involves the excitation of the electron occupying the $s(F_{5c})$ vacancy state to states with mixed Cu $4sp$ and vacancy empty states character. The lowest excitation predicted by the CASPT2 method has a similar physical character but it appears at somewhat lower energy, 1.22 eV. Both methods predict this excitation at energies lower than for a surface F

center since here the vacancy levels are pushed towards the bottom of the conduction band by the interaction with the Cu $4s$ orbital. However, one must notice that the resulting excited state falls within the MgO conduction band and has quite diffuse character, two conditions where both the cluster model approximation and the TD-DFT approach start to fail. For this reason, the prediction of these transitions in the 1.3–1.9 eV range must be considered with some care.

To summarize this section, we have shown how various mechanisms can significantly affect the optical transitions of an adsorbed Cu atom on the MgO surface and we have done a tentative assignment of the experimentally reported EELS spectra of Cu_1/MgO .^{9,10} In the following we extend this analysis to the case of very small Cu aggregates.

B. Cu_2 dimer

The Cu_2 molecule has a $^1\Sigma_g^+$ ground state in gas phase, separated by 1.90 eV from the lowest triplet, $^3\Sigma_u^+$.⁴³ The calculated bond length, 2.26 Å, dissociation energy per atom, $D_e/2$ at =1.01 eV, and singlet-triplet separation, 1.86 eV, of gas-phase Cu_2 are very close to the experimental values ($r_e = 2.22 \text{ \AA}$, $D_e/2$ at =1.04 eV).⁴⁴ Thus, the ground-state properties of the Cu dimer are properly reproduced by the B3LYP functional. When deposited on the MgO surface the ground state remains singlet, with the triplet being 3.19 eV higher in energy. Thus, all the excitations discussed in the following are singlet to singlet transitions, Table II. The first excitation of Cu_2 involves a $\sigma_g \rightarrow \sigma_u^*$ transition where σ_g and σ_u^* are the bonding and antibonding combinations of the Cu $4s$ orbitals. The $\sigma \rightarrow \sigma^*$ transition in TD-DFT occurs at 2.89 eV and has an oscillator strength $f = 0.177$; in CASPT2, $T_e = 2.49 \text{ eV}$ is slightly smaller. Experimentally, the lowest excited singlet state, $^1\Sigma_u^+(\sigma_g \rightarrow \sigma_u^*)$, lies at 2.70 eV above the ground state.⁴⁵ $3d \rightarrow \sigma^*$ transitions have been observed experimentally⁴⁶ or predicted theoretically⁴⁷ to occur at higher energies than the $\sigma_g \rightarrow \sigma_u^*$ one (around 3.1–3.2 eV). This kind of transition, with little intensity, is found also at the TD-DFT level, but the corresponding energy is $T_e = 2.53 \text{ eV}$. The fact that the $3d \rightarrow \sigma^*$ transition in TD-DFT (2.53 eV) is lower than the $\sigma \rightarrow \sigma^*$ one (2.89 eV) could reflect a multireference character of the corresponding excited state which is not properly described by this computational approach. In fact, CASPT2 calculations support this view and properly predict the transition at 2.83 eV, thus at a higher T_e than the $\sigma \rightarrow \sigma^*$ transition, in agreement with experiment.

The geometry of supported Cu_2 is similar on a MgO terrace or step: compared to gas phase, there is an elongation of the Cu-Cu bond by 0.03–0.04 Å only. This reflects the moderate interaction of the Cu dimer with the surface with binding energies of 1.44 eV on the terrace and 1.87 eV on the step, Table II (both values are overestimated by the BSSE). The molecule interacts with a surface oxygen atom and is oriented normal to the surface (terrace) or forms an angle of about 45° with the surface normal (step), see Figs. 1(a) and 1(b). The same configuration of Cu_2 on a MgO terrace site has been found by Musolino, Selloni, and Car with a periodic Car-Parrinello approach.³⁰ On a step, Cu_2 in triplet state interacts with both the O_{5c} and O_{4c} sites, a ge-

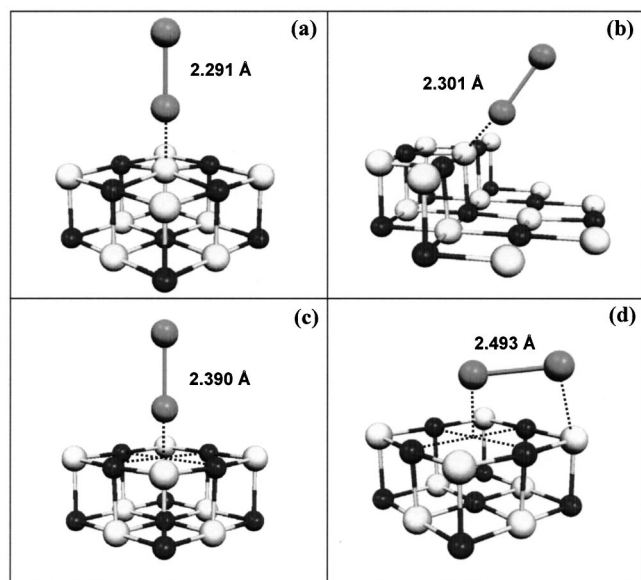


FIG. 1. Structure of a Cu_2 dimer adsorbed on the MgO surface. (a) Terrace site; (b) step site; (c) F center (singlet ground state); (d) F center (triplet).

ometry which is unstable for the singlet configuration. On an F center Cu_2 assumes a normal orientation similar to that found for a terrace, with one Cu atom close to the vacancy and the other pointing outside the surface, Fig. 1(c). The binding of Cu_2 to an F center is stronger than on a terrace, Table II, and the Cu-Cu bond is elongated by 0.13 Å compared to gas phase. Also in this case a different geometry is found for the triplet, Fig. 1(d): the dimer is now tilted with one atom above the vacancy and the second one pointing towards an oxygen ion around the cavity. Also on an F center, however, the triplet state is higher in energy and will not be considered any further.

We consider now the transition energies for the supported Cu dimer. On a terrace, the calculated $\sigma \rightarrow \sigma^*$ transition energy is slightly higher than in the gas phase (2.95 eV versus 2.89 eV) indicating that the relative position of the σ and σ^* levels did not change significantly upon adsorption. This is true also when we consider the step site where the $\sigma \rightarrow \sigma^*$ transition occurs at 2.83 eV, Fig. 2(a). For compari-

son, the $\sigma \rightarrow \sigma^*$ transition of free Cu_2 computed at the Cu-Cu distance of the molecule adsorbed on a step, 2.30 Å, is 2.86 eV, indicating that the change in the Cu-Cu distance has little effect on the transition energy. Thus, the prediction is that a Cu_2 molecule adsorbed on a terrace or a step site will absorb near 2.8–2.9 eV (the corresponding oscillator strength is 0.13–0.14, Table II). Things are more complex for the second transition. On a terrace, a series of absorptions with no intensity has been found around 3.16 eV, Table II. The transitions, which involve the Cu 3d states and the $\text{Cu}_2 \sigma^*$ level, are shifted to higher energies with respect to free Cu_2 . The reason is that the Pauli repulsion of the occupied states on Cu_2 with those of the MgO surface destabilizes the σ and the σ^* levels with largely Cu 4s character, while the localized 3d states are less affected. In this way, the $\sigma \rightarrow \sigma^*$ separation remains more or less unchanged and the corresponding transition is similar to the gas-phase one, while the $3d \rightarrow \sigma^*$ one is shifted to higher energies. This effect is even more pronounced when Cu_2 is bound at a step. Here in fact the $3d \rightarrow \sigma^*$ transitions are even higher, so that in the calculation the second singlet-to-singlet excitation goes from the σ level to diffuse Cu 4s *p* orbitals, Table II, and has some Rydberg character. A comparison with experiment is not simple. In fact, an EELS spectrum has been reported only for Cu_3/MgO , although Cu_2/MgO should have a similar spectrum.^{9,10} A series of bands at 1.7, 2.4, 2.7, 3.2, 3.9, and 5.1 eV has been observed. The problem is complicated by the fact that it is likely that the Cu trimers undergo fragmentation when they are deposited on the surface.

On an F_{5c} center the interaction of Cu_2 takes place by forming a bonding and an antibonding combination between the doubly occupied $s(F_{5c})$ state of the vacancy and the σ^* state of Cu_2 , Fig. 2(b). The consequence of this orbital mixing is a partial charge delocalization of the F center electrons towards the Cu dimer, which explains the elongation of the Cu-Cu bond, Fig. 1(c). The lowest transitions, with no intensity, occur around 2.0–2.2 eV from the doubly occupied level with mixed $s(F_{5c}) + \sigma^*$ character, to the empty $p(F_{5c})$ states of the vacancy. A strong transition is then predicted to occur at 2.85 eV, Table II. This second transition involves as final state a combination of the $p(F_{5c})$ state and the $\text{Cu}_2 4s$ *p* diffuse levels, but, being close to the bottom of the MgO conduction band, it should be considered with some care.

In conclusion, while on a terrace or step sites the $\sigma \rightarrow \sigma^*$ transition of Cu_2 is almost unaffected by the interaction with the oxide surface, on an F center the strong interaction and orbital mixing leads to a completely different optical spectrum. The nucleation of a Cu_2 molecule on F centers should result in a bleaching of the optical transitions typical of this center, although the conclusions about this point are not beyond question.

Before concluding this section, we briefly comment on the energy changes associated to the formation of a MgO supported Cu dimer from the combination of two diffusing Cu atoms on the surface. Dimers represent the first step in nucleation and growth of supported metal clusters.⁴⁸ It has been shown recently that Pd dimers form preferentially at defect sites of the MgO surface.⁴⁹ In fact, defects are good trapping sites where the diffusion of the metal atoms on the

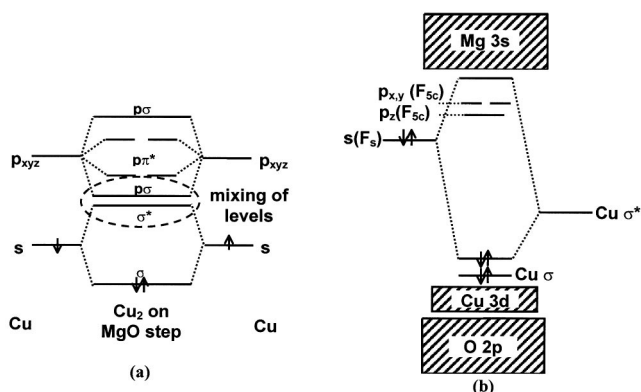


FIG. 2. Schematic representation of the orbital energy diagram for (a) Cu_2 adsorbed on a step, and (b) Cu_2 adsorbed on a F center. Only the most relevant levels involved in the lowest transitions are shown.

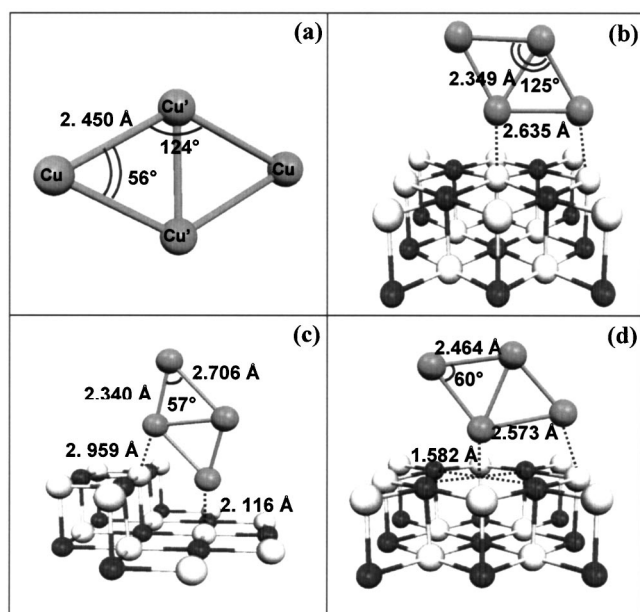


FIG. 3. Structure of a Cu_4 tetramer adsorbed on the MgO surface in its singlet ground state. (a) Gas phase; (b) terrace site; (c) step site; (d) F center.

surface ends. An accurate analysis has shown that divacancies and charged F^+ centers are good sites for Pd dimerization on MgO, while other defects like neutral F centers, or steps can act as nucleation sites only at very low temperature.⁴⁹ To evaluate the tendency of Cu atoms to dimerize on MgO we define E_b , the dimer binding energy, which measures the stability of the adsorbed Cu dimer with respect to two Cu adatoms, one of which is bound on a terrace O_{5c} anion and the other on a specific defect:

$$E_b = -E(\text{Cu}_2/\text{MgO}_{\text{site}}) - E(\text{MgO}_{\text{O}_{5c}}) + E(\text{Cu}_1/\text{MgO}_{\text{site}}) + E(\text{Cu}_1/\text{MgO}_{\text{O}_{5c}}). \quad (1)$$

The computed adsorption energies, E_{ads} in Table I, show that Cu binds more efficiently to a step (1.56 eV) than on a terrace (1.06 eV), and even more strongly to an oxygen vacancy (1.89 eV). However, the dimer binding energy, E_b , Table II, is virtually the same on a terrace (1.33 eV) or on an F center (1.35 eV) and only slightly smaller on a step (1.17 eV). This means that (a) MgO is on always convenient to form a Cu dimer from two Cu adatoms, and (b) dimer formation is independent of the adsorption site and can occur even on the flat terraces. This reflects the fact that the formation of a Cu dimer implies the coupling of two $4s$ electrons with formation of a Cu-Cu σ bond whose strength is not very dependent on the MgO site. In fact, the dimer binding energy on the MgO surface, 1.2–1.3 eV, Table II, is not too different from the Cu_2 dissociation energy in gas phase, 1.14 eV.

C. Cu_4 tetramer

Gas-phase Cu_4 has a rhombic-planar structure, Fig. 3(a), both in its $^1A_g(b_{3u})^2(b_{2u})^0$ and $^3B_{1g}(b_{3u})^1(b_{2u})^1$ electronic states (for the notation we assume a perfect D_{2h} symmetry with the long diagonal of the rhombus oriented along the x direction). In the singlet ground state the Cu-Cu distances,

2.45 Å, are longer than in Cu_2 ; the internal angles are 56° and 124° . In the triplet excited state the distances are 2.40 Å and the angles 70° and 110° . The binding energy per Cu atom is of 1.31 eV, Table III. The ground-state electronic structure is characterized by a series of $3d$ -like states followed by two doubly occupied a_g and b_{3u} levels with bonding and nonbonding character, respectively, formed from combinations of $4s$ and $4p$ Cu orbitals. The lowest unoccupied molecular orbital, LUMO, is a mixture of $4s$ and $4p$ orbitals of b_{2u} symmetry. The HOMO \rightarrow LUMO ($b_{3u} \rightarrow b_{2u}$) transition energy computed at the TD-DFT level is 1.19 eV but does not carry intensity. The next low-lying excited states are almost degenerate and involve a transition from the localized $3d$ states to the b_{2u} LUMO of Cu_4 : they appear ~ 2.80 eV and have appreciable intensity ($f = 0.102$). This kind of excitation has been observed experimentally for matrix-isolated Cu tetramers by Moskovits and Hulse⁴⁶ who assigned the optical absorption measured at 2.92–3.07 eV to a $3d \rightarrow 4s$ transition.

Cu_4 binds much more strongly to MgO than the monomer or the dimer. On regular or step sites the adhesion energy is of about 2.3 eV, while on an F center is of 3.45 eV, Table III. In all cases the ground state remains singlet, and the structure does not deviate markedly from that of the gas phase, remaining pseudorhombic, Figs. 3(b) and 3(c). One edge of the Cu_4 cluster is nearly on top of two oxide anions of the surface; this configuration is the same as found by Musolino, Selloni, and Car³⁰ from Carr-Parrinello simulations. On a step, this involves both the O_{4c} site on the step and the O_{5c} anion in the basal plane; on an F center one Cu atom occupies the center of the vacancy, while the second binds to an O anion at the border of the vacancy, Fig. 3(d). The bonding to the substrate causes a ~ 0.1 Å elongation of the Cu-Cu bond of the cluster edge in direct contact with the MgO surface and much less on the opposite side although the internal angles remain close to 60° . The fact that even on the F center there is only a slight elongation of the Cu-Cu bonds is not in contrast with the possible occurrence of a partial charge transfer from the vacancy to the cluster as found for the Cu_2 dimer. In fact, the ground-state structure of a free Cu_4 cluster anion remains rhombic with Cu-Cu distances nearly identical to those of the neutral form, $r(\text{Cu-Cu}) = 2.45$ Å. Notice that the structure of supported Cu_4 in a triplet state is generally not very distorted compared to the singlet one. An exception is that of an F center where triplet Cu_4 assumes a tetrahedral shape with one apex of the tetrahedron pointing towards the cavity.

On a terrace site, the HOMO \rightarrow LUMO transition of Cu_4 occurs at 1.76 eV and has no intensity. The transition energy is higher than in gas phase (1.19 eV) because the $4s$ - $4p$ empty states are shifted to higher energies by the Pauli repulsion with the substrate. This is clearly shown by a plot of the HOMO and LUMO densities for a free Cu_4 cluster and for the same cluster supported on the MgO terrace, Fig. 4. The plot shows the polarization of the Cu_4 orbitals away from the surface as a consequence of the Pauli repulsion. For the same reason, also the transition from the localized $3d$ levels to the empty $4s$ - $4p$ states is shifted to higher energies, out of the range of the transitions studied in the present

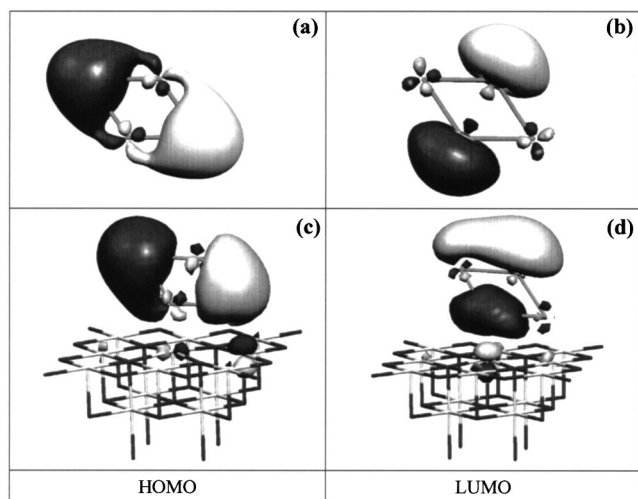


FIG. 4. Plot of the b_{3u} (HOMO) and of the b_{2u} (LUMO) orbitals of free Cu_4 —(a) and (b)—and of Cu_4 supported on the MgO terrace, (c) and (d).

work. The consequence is that the second low-lying singlet excited state is found at 2.61 eV above the ground state; the excitation goes from the HOMO to $4s$ - $4p$ empty orbitals with antibonding character. The transition has a strong intensity ($f=0.448$), Table III. We have computed the lowest T_e of gas phase Cu_4 using the geometry of the supported cluster, but the computed value, 1.16 eV, is very close to that of the fully optimized gas-phase cluster, 1.19 eV. This shows unambiguously that the modification of the Cu_4 optical properties is a direct consequence of the electronic interaction with the substrate (in particular the Pauli repulsion), and not of the change in geometry.

These results are confirmed by the analysis of the transitions of Cu_4 bound at a step site. Here the geometry is even more distorted than on a terrace site, with two of the Cu-Cu edges expanded up to 2.71 Å, Fig. 3(c). The interaction with MgO leads to a destabilization of the Cu_4 empty states which are shifted towards the bottom of the MgO conduction band. As a result, these states are mixed in with the Mg $3s$ states of the low-coordinated Mg cations which contribute to the bottom of the MgO conduction band. The HOMO→LUMO transition occurs at 1.42 eV and, as for free Cu_4 and for Cu_4 supported on terrace sites, has no intensity. The next transition is similar to that of Cu_4 on MgO terraces, as it occurs at 2.58 eV and has a strong intensity ($f=0.395$). As for Cu_2 , also in this case we have to mention that the partial mixing with empty Mg states indicates a delocalized character of the transition, so that the computed T_e values must be taken with some care.

On the F_{5c} center the geometry is not much distorted compared to gas phase and, as pointed out above, the major change is the elongation to 2.57 Å of the Cu-Cu bond at the interface, Fig. 3(d). The presence of a metal cluster with four $4sp$ valence electrons and of two electrons trapped in the vacancy introduces a number of states in the MgO gap, Fig. 5. These states are higher in energy than the Cu $3d$ states which are found just above the top of the O $2p$ valence band. The Cu $4sp$ empty levels and the doubly occupied $s(F_{5c})$ state are strongly mixed, Fig. 5, with partial charge transfer

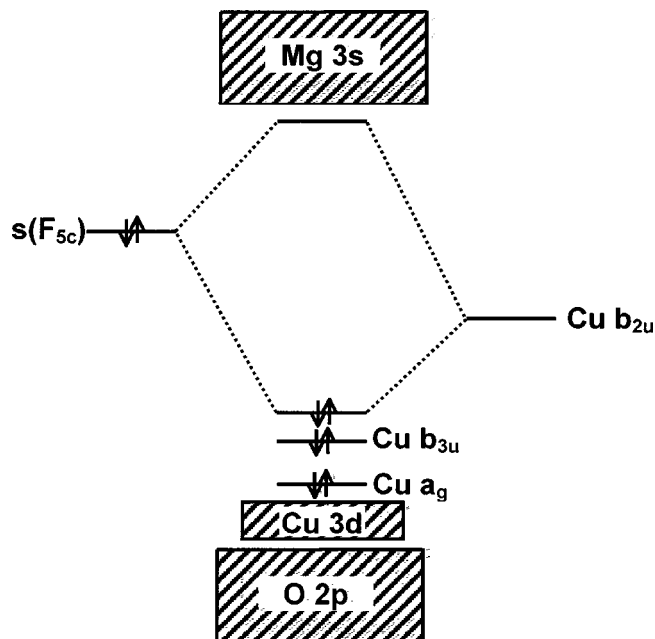


FIG. 5. Schematic representation of the orbital energy diagram for Cu_4 adsorbed on an F center. Only the most relevant levels involved in the lowest transitions are shown.

from the vacancy to Cu_4 , so that the analysis of the transitions on this system is less straightforward than in previous cases. The lowest singlet→singlet (HOMO→LUMO) transition occurs from the bonding combination of the vacancy level with the Cu_4 b_{2u} LUMO to the corresponding antibonding combination; this is $(F_{5c}) + b_{2u}(4sp) \rightarrow s(F_{5c}) - b_{2u}(4sp)$, with a transition energy of 1.92 eV but zero intensity. Another transition is found with similar character but the excited state has both $s(F_{5c})$ and Cu $5s$ (Rydberg) character. The corresponding T_e is 2.51 eV and the oscillator strength is 0.131, Table III. Also in this case the transition energy for the unsupported Cu_4 cluster at the same geometry obtained on the F center is 1.01 eV, much closer to that of gas-phase Cu_4 , 1.19 eV, than to the value for $\text{Cu}_4/\text{MgO}(F_{5c})$, 1.92 eV, Table III. This confirms that the changes in optical properties depend more on the electronic interaction with the oxide than on the changes in geometry upon adsorption.

IV. CONCLUSIONS

In this work we have considered the optical properties of Cu monomers, dimers, and tetramers deposited on various sites of the MgO surface. In particular, the study has been done for metal atoms and clusters adsorbed on a (100) terrace, on an extended defect such as a step, and on a point defect such as the neutral oxygen vacancy (F center). While this is far from providing a complete mapping of the interaction of a Cu cluster with the various defects of the MgO surface,⁵⁰ it gives a first basis to rationalize the effects which determine changes in the optical transitions of a metal cluster deposited on an oxide support. To this end, also the optical properties of the corresponding free clusters have been considered. The calculations have been performed at the TD-DFT level using the hybrid B3LYP functional. For the gas-

phase clusters and for a few simple cases of supported species the calculations have been done also using the sophisticated wave function based CASPT2 approach. Unfortunately, the use of this method is restricted to cases where the number of electrons and orbitals included in the active space is limited. Still, from the comparison of the TD-DFT and CASPT2 results with the existing experimental data we obtained a validation of the results for the larger and more complex systems studied only at the TD-DFT level.

The results can be summarized in the following main conclusions.

(1) The results for isolated Cu atoms deposited on MgO help to assign the bands in the EELS spectra of Schaffner *et al.*^{9,10} Different from what has been proposed originally, i.e., that the feature at 2.7 eV is due to Cu⁺ ions, we suggest that this band is due to the $4s \rightarrow 4p$ transition of the neutral Cu atoms stabilized on the oxide anions of the MgO terraces (the calculated value is 2.6 eV). In gas phase the allowed transition occurs at 3.9 eV. The fact that on the oxide surface the transition is red shifted by 1.3 eV is a sign of the electronic changes induced on the metal upon adsorption.

(2) The geometry of Cu dimers and tetramers changes slightly by effect of the interaction with the substrate. This is not necessarily the case for all atoms and for all substrates and reflects the fact that the Cu-Cu bonds are stronger than the Cu-MgO ones. However, this helps in separating geometric from electronic effects in the analysis of the changes in optical properties going from free to supported clusters. The results show in fact that the geometrical changes have a much smaller effect on the transitions than the interface bonding. This depends on the site where the cluster is adsorbed, but in general the Pauli repulsion shifts the Cu $4sp$ filled and empty levels to higher energies. This effect dominates the interaction with terrace and step sites. Here the Cu cluster levels are well separated from the MgO valence band and conduction band states, and the main effect on the electronic structure is related to the polarization of the cluster orbitals induced by the support.

(3) On the F centers the presence of states in the gap of the oxide leads to a strong mixing with the states of the Cu atom or of the Cu clusters. This changes completely the nature of the low-lying transitions and their energies. These strong interactions do not deeply modify the geometry of the adsorbate, but change significantly the electronic structure, with partial charge transfer from the vacancy to the adsorbed cluster. As a consequence, both the optical properties of the isolated F center and of the Cu₄ cluster are lost and replaced by a series of transitions which involve states with mixed character.

ACKNOWLEDGMENTS

Financial supports from the Italian Ministero dell'Istruzione, Università e Ricerca, through a COFIN project, from the Spanish Ministerio de Ciencia y Tecnología Project No. BQU2002-04029-C02-01, and from the Generalitat de Catalunya (Project No. 2001SGR-00043 and Distinció de la Generalitat de Catalunya per a la Promoció de la Recerca Universitària awarded to F.I.) are acknowledged.

Computer time was in part provided by the CESCA, CEPBA, CIRI, and CINECA supercomputer centers.

- ¹H.-J. Freund, *Surf. Sci.* **500**, 271 (2002).
- ²S. Abbet, E. Riedo, H. Brune, U. Heiz, A. M. Ferrari, L. Giordano, and G. Pacchioni, *J. Am. Chem. Soc.* **123**, 6172 (2001).
- ³U. Heiz and W. D. Schneider, *J. Phys. D* **33**, R85 (2000).
- ⁴A. Sanchez, S. Abbet, U. Heiz, W. D. Schneider, H. Häkkinen, R. N. Barnett, and U. Landman, *J. Phys. Chem. A* **103**, 9573 (1999).
- ⁵L. Giordano, G. Pacchioni, F. Illas, and N. Rösch, *Surf. Sci.* **499**, 73 (2002).
- ⁶A. Mie, *Ann. Phys. (Leipzig)* **25**, 377 (1908).
- ⁷N. Nilius, N. Ernst, and H. J. Freund, *Phys. Rev. Lett.* **84**, 3994 (2000).
- ⁸T.-H. Lee and R. M. Dickson, *Proc. Natl. Acad. Sci. U.S.A.* **100**, 3043 (2003).
- ⁹M. H. Schaffner, F. Patthey, W. D. Schneider, and L. G. M. Pettersson, *Surf. Sci.* **402-404**, 450 (1998).
- ¹⁰M. H. Schaffner, F. Patthey, and W. D. Schneider, *Eur. Phys. J. D* **9**, 609 (1999).
- ¹¹M. Petersilka, U. J. Gossmann, and E. K. U. Gross, *Phys. Rev. Lett.* **76**, 1212 (1996).
- ¹²K. Andersson, P. A. Malmqvist, B. O. Roos, A. J. Sadlej, and K. Wolinski, *J. Phys. Chem.* **94**, 5483 (1990).
- ¹³K. Andersson, P. A. Malmqvist, and B. O. Roos, *J. Phys. Chem.* **96**, 1218 (1992).
- ¹⁴A. D. Becke, *J. Chem. Phys.* **98**, 5648 (1993).
- ¹⁵C. Lee, W. Yang, and R. Parr, *Phys. Rev. B* **37**, 785 (1988).
- ¹⁶J. M. Matxian, A. Irigoras, J. E. Fowler, and J. M. Ugalde, *Phys. Rev. A* **63**, 013202 (2000).
- ¹⁷K. Raghavachari, D. Ricci, and G. Pacchioni, *J. Chem. Phys.* **116**, 825 (2002).
- ¹⁸C. de Graaf, R. Broer, and W. C. Nieuwpoort, *Chem. Phys.* **208**, 35 (1996).
- ¹⁹C. de Graaf and R. Broer, *Phys. Rev. B* **62**, 702 (2000).
- ²⁰C. Sousa, C. de Graaf, and G. Pacchioni, *J. Chem. Phys.* **114**, 6259 (2001).
- ²¹C. Sousa, C. de Graaf, F. Illas, M. T. Barriuso, J. A. Aramburu, and M. Moreno, *Phys. Rev. B* **62**, 13366 (2000).
- ²²K. Andersson, M. Barysz, A. Bernhardsson *et al.*, MOLCAS version 5.2, University of Lund, Sweden, 2000.
- ²³*Cluster Models for Surface and Bulk Phenomena*, NATO Advanced Studies Institute, Series B: Physics, edited by G. Pacchioni, P. S. Bagus, and F. Parmigiani (Plenum, New York, 1992), Vol. 283.
- ²⁴G. Pacchioni, A. M. Ferrari, A. M. Marquez, and F. Illas, *J. Comput. Chem.* **18**, 617 (1996).
- ²⁵A. M. Ferrari and G. Pacchioni, *Int. J. Quantum Chem.* **58**, 241 (1996).
- ²⁶G. Pacchioni and N. Rösch, *J. Chem. Phys.* **104**, 7329 (1996).
- ²⁷I. Yudanov, G. Pacchioni, K. Neyman, and N. Rösch, *J. Phys. Chem. B* **101**, 2786 (1997).
- ²⁸N. Lopez, F. Illas, N. Rösch, and G. Pacchioni, *J. Chem. Phys.* **110**, 4873 (1999).
- ²⁹A. V. Matveev, K. Neyman, and I. Yudanov, *Surf. Sci.* **426**, 123 (1999).
- ³⁰V. Musolino, A. Selloni, and R. Car, *Phys. Rev. Lett.* **83**, 3242 (1999).
- ³¹P. J. Hay and W. R. Wadt, *J. Chem. Phys.* **82**, 299 (1985).
- ³²R. Ditchfield, W. Hehre, and J. A. Pople, *J. Chem. Phys.* **54**, 724 (1971).
- ³³A. M. Ferrari, R. Soave, A. D'Ercole, C. Pisani, E. Giamello, and G. Pacchioni, *Surf. Sci.* **83**, 479 (2001).
- ³⁴S. Boys and F. Bernardi, *Mol. Phys.* **19**, 553 (1970).
- ³⁵N. Lopez, F. Illas, and G. Pacchioni, *J. Phys. Chem. B* **103**, 1712 (1999).
- ³⁶M. J. Frisch *et al.*, GAUSSIAN98, Revision A.6, Gaussian Inc., Pittsburg PA, 1998.
- ³⁷F. Illas and G. Pacchioni, *J. Chem. Phys.* **108**, 7835 (1998).
- ³⁸J. E. Sansonetti, W. C. Martin, and S. L. Young (2004), Handbook of Basic Atomic Spectroscopic Data (version 1.1). [Online] Available: <http://physics.nist.gov/Handbook> [2004, September 10]. National Institute of Standards and Technology, Gaithersburg, MD.
- ³⁹A. A. Radzig and B. M. Smirnov, *Reference Data on Atoms Molecules and Ions* (Springer, Berlin, 1985).
- ⁴⁰A. M. Ferrari and G. Pacchioni, *J. Phys. Chem.* **99**, 17010 (1995).
- ⁴¹C. Sousa, G. Pacchioni, and F. Illas, *Surf. Sci.* **429**, 217 (1999).

- ⁴²J. Kramer, C. Tegenkamp, and H. Pfnür, *Phys. Rev. B* **67**, 235401 (2003).
- ⁴³V. E. Bondybey, *J. Chem. Phys.* **77**, 3771 (1982).
- ⁴⁴J. Ho, K. M. Ervin, and W. C. Lineberger, *J. Chem. Phys.* **93**, 6987 (1990).
- ⁴⁵K. P. Huber and G. Herzberg, *Constants of Diatomic Molecules* (Van Nostrand, New York, 1981).
- ⁴⁶M. Moskovits and J. E. Hulse, *J. Chem. Phys.* **67**, 4271 (1977).
- ⁴⁷M. Witko and H.-O. Beckmann, *Mol. Phys.* **47**, 945 (1982).
- ⁴⁸G. Haas, A. Menck, H. Brune, J. V. Barth, J. A. Venables, and K. Kern, *Phys. Rev. B* **61**, 11105 (2000).
- ⁴⁹L. Giordano, C. Di Valentin, J. Goniakowski, and G. Pacchioni, *Phys. Rev. Lett.* **92**, 096105 (2004).
- ⁵⁰G. Pacchioni, *Chem Phys Chem* **4**, 1041 (2003).